

H on Pt(110): An atypical chemisorption site at low coverages

Z. Zhang, M. Minca, C. Deisl, T. Loerting, A. Menzel,* and E. Bertel
Institute of Physical Chemistry, University of Innsbruck, A-6020 Innsbruck, Austria

R. Zucca and J. Redinger

Center for Computational Materials Science, Vienna University of Technology, A-1060 Vienna, Austria

(Received 9 June 2004; published 15 September 2004)

The use of hydrogen-modified Pt(110) as a template for the growth of one-dimensional adsorbate structures motivated our investigation of this surface with quantitative low-energy electron diffraction (LEED) and density functional theory (DFT) calculations. The analysis reveals a strong coupling of the H atom positions to Pt lattice relaxations on the (1×2) missing row surface. Contrary to all former assignments, we conclude from the experiment that at low coverages (β_2 state) H occupies adsorption sites above the outermost close-packed rows. This is supported by DFT calculations, which identify the short-bridge site on the outermost row as the preferred chemisorption site.

DOI: 10.1103/PhysRevB.70.121401

PACS number(s): 68.43.Bc, 82.65.+r

Low dimensional materials display a rich and technologically highly interesting phase diagram.¹ The dimensionality determines the strength of many-body effects and consequently the macroscopic materials properties.^{2,3} Strongly anisotropic single crystal surfaces and their adsorbate-covered, reconstructed or stepped modifications are promising templates for the design and characterization of one-dimensional systems on surfaces.⁴⁻⁶ One of these model templates is the β_2 -hydrogen-modified Pt(110)(1×2) missing-row surface, on which adsorbates with one-dimensional electronic band structure can be grown, whereas the clean (1×2) missing row surface supports only a two-dimensional adsorbate system.^{7,8} In addition the H/Pt(110) system is known to be an excellent model system for Pt particles in H fuel cells.^{9,10} A precise knowledge of H bonding geometry and energetics is therefore mandatory for a detailed understanding of both the quasi-one-dimensional properties of H/Pt(110) and the technological application of Pt in fuel cells and catalysis.

Up to now, there is still considerable disagreement as to the chemisorption site of H on Pt(110). The usual assumption of highly coordinated hydrogen^{11,12} sitting in the deep troughs of the missing rows was supported by work function measurements^{13,14} and vibrational spectroscopy,¹⁵ but was challenged by the first direct structure-probing experiment (Helium atom scattering, HAS), which led to the proposal of a highly coordinated subsurface site.¹⁶ Quite contrary to all these proposals, we show in this Rapid Communication experimental and theoretical evidence that β_2 -H chemisorbs at the *low coordinated* short bridge site on top of the outermost platinum rows. This is the first observation of such a behavior on a fcc metal surface. It underlines a peculiar behavior of Pt with respect to chemical bond formation, setting it apart from the isoelectronic transition metals Ni and Pd.^{17,18}

The experiments were carried out in an ultra high vacuum system with 5×10^{-11} mbar base pressure. The sample, a precisely oriented Pt(110) single crystal (miscut $< 0.1^\circ$), was mounted on a liquid-N₂ reservoir. The sample was cleaned by Ar sputtering and annealing at 1020 K followed by three cycles of 3 L O₂ adsorption at 130 K (saturation)

and subsequent flash desorption (3 K/s) to 920 K. Hydrogen or deuterium were dosed by backfilling the experimental chamber at crystal temperatures around 130 K. The well known β_2 and β_1 adstates^{9,13,14,19} are fully occupied after exposures of 0.6 and 240 L, respectively. The controversially discussed α -peak^{9,14,19,20} at around $T=185$ K appears additionally in our temperature programmed desorption (TPD) spectra after hydrogen or deuterium exposures above ~ 266 L (1×10^{-6} mbar H₂ for 200 s). A study of the coverage dependence of TPD and LEED experiments will be given in a separate paper.²¹

The LEED- I/V data were recorded using a CCD camera operated under computer control (AIDA-PC),²² integrated spot intensities were obtained from $I(E)$ spectra. A sharp missing-row (1×2) LEED pattern was visible after hydrogen exposures below 240 L. The data were taken at low temperatures (130 K) and in steps of 0.5 eV, from 50 to 500 eV for normal incidence of the primary beam. For the retrieval of structural data from the measured $I(E)$ spectra the perturbation method tensor LEED²² was applied using the TensErLEED program package.²³ More details are given in Ref. 24. The accumulated data base width of spot intensities in the range of 50 to 500 eV amounts to $\Delta E_i = 2839$ eV and $\Delta E_f = 3374$ eV for integer and fractional order beams, respectively. Since the hydrogen atoms can be neglected due to their extremely low scattering factor, both clean and hydrogen-modified surfaces were treated with exactly the same setup of the TensErLEED program.

First principles density functional theory (DFT) calculations have been performed with the projector augmented wave Vienna ab-initio simulation Package (VASP).²⁵ Exchange-correlation was treated within the generalized gradient approximation (GGA),²⁶ yielding a bulk lattice constant of 3.984 Å. Repeated slabs of 11 Pt layers with an ad-layer of H atoms on the missing Pt-row side and a $p(1 \times 1)$ Pt termination on the other side were separated by a 12-Å thick vacuum layer. All layers were relaxed except three layers of the Pt substrate on the far side frozen to the relaxed geometry of a $p(1 \times 1)$ Pt(110) surface. An energy

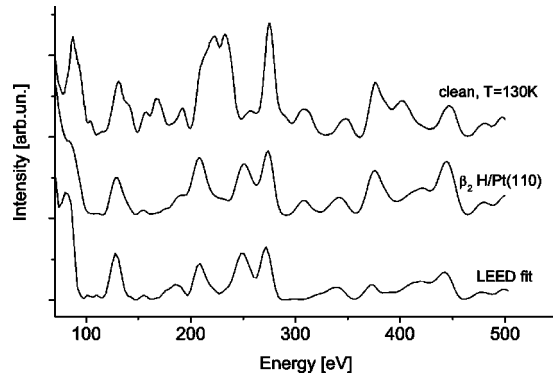


FIG. 1. I/V curves for the $(1,1/2)$ beam of the clean and β_2 -H-modified surface together with the best-fit calculation.

cutoff of 250 eV and an $8 \times 8 \times 1$ Monkhorst-Packtype k -point mesh was sufficiently accurate for the present purposes.

Both the clean and hydrogen-covered surfaces are known to be missing row reconstructed.¹³ However, Fig. 1 shows the considerable differences observed in the I/V curves of the clean and hydrogen-modified Pt(110) surface, indicating a substantial structural change in the surface geometry. The geometry parameters changed during the structural search are indicated in Fig. 2: The first five interlayer distances d_{12} to d_{56} , the vertical bucklings b_3 and b_5 of the third and fifth layers, the lateral pairing amplitudes p_2 and p_4 between

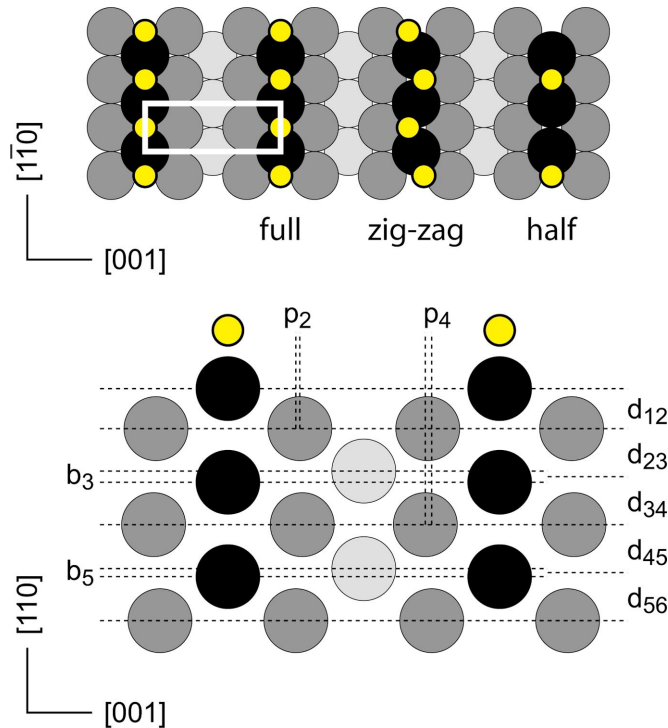


FIG. 2. (Color) Model of the Pt atom geometry on clean and hydrogen-modified $H/Pt(110)(1 \times 2)$ surfaces with structural parameters determined. Typical H atom (yellow) arrangements used in the DFT calculations are denoted as full (β_2 -H), zig-zag (slightly distorted β_2 -H to elucidate the effects of low energy lateral H displacements), and half (half-filled β_2 -H), respectively.

TABLE I. Experimental and theoretical parameters for the missing-row structure of the clean (Ref. 24) and hydrogen-modified β_2 -H/Pt(110)(1×2) surface (this work). $d_{i,i+1}$ denotes the (average) inter-layer spacing, while p_i and b_i denote the lateral pairing and buckling in layer i (all values in Å). Error limits for the parameters derived by the present LEED analysis (neglecting parameter correlations) are ± 0.02 Å for $\Delta d_{i,i+1}$, ± 0.05 Å for b_i and ± 0.07 Å for p_i . DFT: full: all bridge sites filled, zig-zag: hydrogens displaced by 0.4 Å toward microfacets, half: every second site empty. For easier comparison with LEED all DFT values are scaled to the LEED bulk interlayer distance of $d_0 = 1.386$, DFT: $d_0 = 1.409$.

System method Config.	Pt(110)		β_2 -H-Pt(110)		
	LEED Clean	LEED β_2 -H	Full	DFT Zig-zag	DFT Half
d_{12}	1.15	1.25	1.32	1.26	1.22
d_{23}	1.37	1.36	1.33	1.34	1.36
d_{34}	1.41	1.41	1.43	1.42	1.42
d_{45}	1.40	1.38	1.42	1.42	1.42
d_{56}	1.38	1.39	1.36	1.35	1.36
b_3	0.26	0.25	0.31	0.31	0.32
b_5	0.03	0.03	0.06	0.07	0.03
p_2	0.035	0.00	-0.022	0.006	0.004
p_4	0.065	0.05	0.057	0.053	0.064

neighboring atoms in $[001]$ direction within the second and fourth layers, and the (isotropic) vibrational amplitudes v_i of the first three layers ($i=1,2,3$). The inner potential was allowed to vary with energy according to Ref. 24. In order to avoid running into local minima during the fit procedure, the calculations for the hydrogen-modified surface were started both from the clean surface geometry (e.g., $d_{12} = 1.15$ Å) as well as from the considerably different bulk layer distances (e.g., $d_{12} = 1.38$ Å). In both cases, the same best-fit structure with a relaxation in between the two starting points ($d_{12} = 1.25$ Å) was obtained.

Calculated and experimental LEED intensities agree very well for the H-covered surface (see Fig. 1). The calcu-

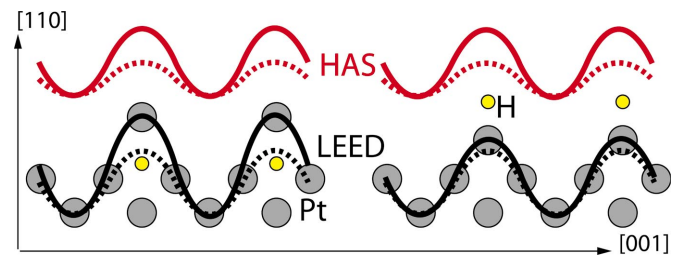


FIG. 3. (Color) Schematic representation of the expected experimental corrugation (HAS, red curves; LEED, black curves) on the hydrogen modified Pt(110) surface. The left part of the figure shows the corrugations in case of hydrogen atoms (yellow) adsorbing below the outermost Pt row, whereas on the right the case of hydrogen adsorbing above the outermost row is shown. The LEED-corrugation follows essentially the Pt atom positions, whereas HAS detects profiles of constant charge density which are smoothed by the Smoluchovsky effect. The smaller corrugation of the clean surface is represented by the dotted lines.

lation with the best fit parameters yields a Pendry- R -factor of $R=0.24$ very similar to the clean surface.²⁴ These seemingly modest R -factors are among the best ever achieved for a fcc(110) surface.²⁴ The best fit parameters for the β_2 -H/Pt(110)-(1 \times 2) surface are given in Table I together with the results of the DFT calculation. For comparison, we also provide the values for clean H/Pt(110)(1 \times 2).²⁴

The most important change upon hydrogen adsorption is the relaxation in the first interlayer spacing d_{12} . The change amounts to 0.10 Å, well exceeding the combined error limits of both experiments. The other interlayer spacings and the considerable buckling in the third layer stay roughly the same within experimental errors. According to the LEED calculation, the vibrational amplitude of the outermost platinum atoms increases by a factor of 1.5 upon hydrogen adsorption ($v_1=0.16$ Å). The enhanced vibrational amplitude is consistent with the outward movement of the top-layer Pt atoms both indicating a softer binding potential. A refined analysis would require the use of anisotropic vibrational amplitudes which, however, is beyond the scope of this work.

We stress that the substantial change of relaxation (+0.1 Å) observed here is much less than the corrugation change (+0.5 Å) observed in the HAS experiment by Kirsten *et al.*¹⁶ This difference in corrugation and relaxation measured in the HAS and LEED experiments, respectively, is precisely the experimental information pinpointing the adsorption site of the β_2 -hydrogen on Pt(110). As shown in Fig. 3, these experiments probe the geometry of the charge density at a very different level. The LEED electrons are scattered by the ion cores of the platinum atoms. The dominant interaction here is the Coulomb potential. The helium atoms, in contrast, probe approximately contours of constant valence electron density at low charge density levels outside the surface. The dominant interaction is the Pauli repulsion, preventing substantial overlap between the He and the substrate charge clouds. In the case of hydrogen chemisorbed in a subsurface site below the outermost Pt row (Fig. 3, left), the large change in corrugation measured by HAS would indicate a similar change in the outermost Pt-atom positions,¹⁶ which is not consistent with the present LEED results. However, in the case of hydrogen adsorbing on top of the outermost row (top and/or short-bridge sites), the change in valence density corrugation is due to both the position change of platinum atoms *plus* the hydrogen-induced electron density, whereas the LEED experiment measures the (smaller) change in the Pt-atom positions (Fig. 3, right). Thus only chemisorption sites above the outermost rows are consistent with the combined experimental evidence from LEED and HAS.

This conclusion is corroborated by our DFT calculation of the adsorption geometry. In order to explore the dependency of the relaxation on coverage and H atom position, 44 different geometries were calculated. Generally, the calculation shows that both small H displacements from the ideal short bridge site and lower coverage lead to a lowering of the interlayer spacing (see some examples in Fig. 2 and Table I). Comparing the “full” and “zig-zag” models reveals that an H atom position shift of just 5% of the unit cell width toward the (111) facet costs merely 46 meV but results in a decrease

of the interlayer spacing by 5%, showing a strong coupling of relaxation and H atom position. The strong coupling to both the hydrogen position and coverage is obviously the reason for the slightly smaller interlayer spacing measured by LEED as compared to the ideal $T=0$ K fully occupied short bridge geometry calculated. Hydrogen positions on the facets or in the trough give a much smaller $d_{12}=1.10$ Å not consistent with the experiment. The same picture emerges from the calculated total energies: The short-bridge site on the outermost row is about 115 meV lower in total energy than the on-top site in agreement with Ref. 27. The octahedral and tetrahedral subsurface sites below the outermost row are unstable against molecular desorption, the energy difference to the short bridge-site amounting to 1.3 and 1.0 eV, respectively. Sites inside the trough are energetically (276 to 560 meV) in between the sites on top of the row and the subsurface site. On the (111) facets, the low coordinated site on top of the second layer Pt atoms (80 meV) is preferred over the higher coordinated sites (130 to 180 meV). Interestingly, and in agreement with experiment,¹³ the DFT calculation yields a small nearest neighbor attraction for hydrogen adatoms in the top-row bridge site. Thus, with increasing coverage, hydrogen occupies first all short bridge sites (β_2 state) before the sites in the troughs/microfacets are occupied (β_1 state).

This is consistent with the experimental HAS and LEED data at higher coverage: The filling of the sites in the troughs/microfacets results in a lowering of the corrugation as measured by HAS,¹⁶ while the I/V curves measured by LEED (not shown) are virtually identical. In passing we note that the identical I/V curves for the high coverage phases and the low coverage phase justify our assumption of negligible scattering cross section of the hydrogen *a posteriori*.

The seemingly contradicting interpretations of other experiments can be resolved within the present model. The small energy difference (115 meV) between on-top and short bridge site above the outermost row and the microfacets (80 meV) allows large vibrational motions and a high diffusivity of the hydrogen atoms along the row. This might explain the relatively small corrugation along the row measured by HAS which was taken as counter-evidence for the short bridge site.¹⁶

Our results actually confirm an HREELS experiment of H/Pt(110)¹⁵ indicating a two-fold bridge site at low coverage, which, however, was misinterpreted as an adsorption site within the deep troughs. Generally, interpretations of experimental results from indirect methods^{13,14,28,29} have to be viewed with caution. With respect to the work function measurements,^{13,14} for instance, a recent overview of hydrogen on metals concludes that “the structural influence of hydrogen is accompanied by a redistribution of electronic charges within the surface leading to unforeseen changes of the electronic work function.”³⁰ In agreement with Ref. 13 we find that preadsorption of 0.5 L CO removes the β_2 peak from the hydrogen-TDS spectra, whereas the β_1 state seems to be unaffected. This confirms our model since CO is known to adsorb on top of the outermost Pt rows, too.³¹ In the present model the small H induced work function change simply indicates a rather covalent bonding. The bonding of H to metal surfaces can be rationalized to a large degree by

assuming that the proton seeks an optimum embedding into an appropriate diffuse charge density. This is most easily achieved in a highly coordinated adsorption site. In fact, the most stable bonding site of H on Ni(110) and Pd(110) is the fcc pseudo-threefold site at the (111) microfacets of the (110) surface.^{17,18} The strikingly different behavior observed on Pt(110) is a consequence of a directional covalent bond formation with Pt *d*-orbitals. The different bonding characteristic results from the relativistic contraction of the inner *s*-orbitals and the concomitant *d*-shell expansion. This exposes the *d*-orbitals in Pt, making them more readily available for a directional covalent bond as compared to the 3*d* and 4*d* transition metals. We found a similar behavior for Br/Pt(110)³² and also in a comparative study of CO-bonding on the transition metal surfaces.³³

In conclusion, the present study reveals the first case where on a fcc transition metal a low-coordinated short bridge site is the most stable chemisorption site of H. We find a substantial derelaxation of the Pt(110) substrate and a strong coupling of the Pt lattice relaxation to the H atom position. In general and simplified terms, the β_2 -H-modified Pt(110) surface represents a better template for 1D growth of adsorption systems than the clean Pt(110) surface since, on the one hand, adsorption sites above the rows are blocked for coadsorbates with less binding energy. On the other hand, the small radius of the hydrogen atom still allows adsorption of 1D chains of the coadsorbate in the troughs.

Support of this work by the Austrian Science Fund is gratefully acknowledged.

*Corresponding author; electronic address: alexander.menzel@uibk.ac.at

¹M. Imada, A. Fujimori, and Y. Tokura, *Rev. Mod. Phys.* **70**, 1039 (1998).

²J. Voit, *Rep. Prog. Phys.* **57**, 977 (1994).

³T. Valla, P. D. Johnson, Z. Yusof, B. Wells, Q. Li, S. M. Loureiro, R. J. Cava, M. Mikami, Y. Mori, M. Yoshimura, and T. Sasaki, *Nature (London)* **417**, 627 (2002).

⁴P. Segovia, D. Purdie, M. Hengsberger, and Y. Baer, *Nature (London)* **402**, 504 (1999).

⁵A. Mugarza, A. Mascaraque, V. Pérez-Dieste, V. Repain, S. Rousset, F. J. García de Abajo, and J. E. Ortega, *Phys. Rev. Lett.* **87**, 107601 (2001).

⁶N. Nilius, T. Wallis, and W. Ho, *Science* **297**, 1853 (2002).

⁷W. Widdra, P. Trischberger, and J. Henk, *Phys. Rev. B* **60**, R5161 (1999).

⁸W. Widdra, *Appl. Phys. A: Mater. Sci. Process.* **72**, 395 (2001).

⁹C. Lu and R. I. Masel, *J. Phys. Chem. B* **105**, 9793 (2001).

¹⁰W. Chrzanowski and A. Wieckowski, *Langmuir* **14**, 1967 (1998).

¹¹G. Burns, *Solid State Physics* (Academic, New York, 1985).

¹²K. Christmann, *Surf. Sci. Rep.* **9**, 1 (1988).

¹³J. R. Engstrom, W. Tsai, and W. H. Weinberg, *J. Chem. Phys.* **87**, 3104 (1987).

¹⁴C. Shern, *Surf. Sci.* **264**, 171 (1992).

¹⁵W. Stenzel, S. Jahnke, Y. Song, and H. Conrad, *Prog. Surf. Sci.* **35**, 159 (1991).

¹⁶E. Kirsten, G. Parschau, W. Stocker, and K. Rieder, *Surf. Sci.* **231**, L183 (1990).

¹⁷G. Kresse and J. Hafner, *Surf. Sci.* **459**, 287 (2000).

¹⁸W. Dong, V. Ledentu, Ph. Sautet, E. Eichler, and J. Hafner, *Surf. Sci.* **411**, 123 (1998).

¹⁹G. Anger, H. F. Berger, M. Luger, A. W. S. Feistritz, and K. D. Rendulic, *Surf. Sci.* **219**, L583 (1989).

²⁰G. Attard, H. Ebert, and R. Parsons, *Surf. Sci.* **240**, 125 (1990).

²¹M. Minca, A. Menzel, and E. Bertel (unpublished).

²²K. Heinz, *Rep. Prog. Phys.* **58**, 637 (1995).

²³V. Blum and K. Heinz, *Comput. Phys. Commun.* **134**, 392 (2001).

²⁴V. Blum, L. Hammer, K. Heinz, C. Franchini, J. Redinger, K. Swamy, C. Deisl, and E. Bertel, *Phys. Rev. B* **65**, 165408 (2002).

²⁵G. Kresse and J. Furthmüller, *Phys. Rev. B* **54**, 11 169 (1996); see also URL: <http://cms.mpi.univie.ac.at/vasp/>; G. Kresse and D. Joubert, *Phys. Rev. B* **59**, 1758 (1999).

²⁶Y. Wang and J. P. Perdew, *Phys. Rev. B* **44**, 13 298 (1991).

²⁷S. Horch, H. T. Lorensen, S. Helveg, E. Laegsgaard, I. Stensgaard, K. W. Jacobsen, J. K. Norskov, and F. Besenbacher, *Nature (London)* **398**, 134 (1999).

²⁸K. Dückers, K. C. Prince, H. P. Bonzel, V. Cháb, and K. Horn, *Phys. Rev. B* **36**, 6292 (1987).

²⁹R. Ducros and J. Fusy, *Surf. Sci.* **207**, L943 (1988).

³⁰K. Heinz and L. Hammer, *Phys. Status Solidi B* **159**, 225 (1997).

³¹R. Sharma, W. Brown, and D. King, *Surf. Sci.* **414**, 68 (1998).

³²A. Menzel, K. Swamy, R. Beer, P. Hanesch, E. Bertel, and U. Birkenheuer, *Surf. Sci.* **454-456**, 88 (2000).

³³E. Bertel, N. Memmel, G. Rangelov, and U. Bischler, *Chem. Phys.* **177**, 337 (1993).